

# Computational Fluid Dynamics and Experimental Investigation of Wrap-Around-Fins Missile Rolling Moment

Emrah Gülay<sup>1)</sup>  
Ali Akgül<sup>1)</sup>  
Jovan Isaković<sup>2)</sup>  
Slobodan Mandić<sup>2)</sup>

The CFD calculations of the rolling moment coefficient by the FLUENT software package and the wind tunnel measurements were performed for two missile models. One missile model is with wrap-around fins and the other missile model is with flat fins. The purpose of this paper is to compare the calculated rolling moment coefficients of the selected missile models by computational fluid dynamics (CFD) to the experimental data. The influence of the turbulence model on the accuracy of the calculated rolling moment is also analyzed. There is better agreement between the calculated and measured rolling moment coefficients in the supersonic regions than in the subsonic regions of Mach numbers. It is proved that the rolling moment coefficient of the missile with wrap-around fins can be written as the sum of the moment due to the curvature of the fins and the moment due to the cant angle of the equivalent flat fins.

*Key words:* aerodynamic testing, aerodynamic calculation, aerodynamic moment, rolling moment, missile, flat fin, wrap-around fin, aerodynamic coefficient, computational fluid dynamics.

## Notation and symbols

- $C_\ell$  – Rolling moment coefficient  
 $C_{\ell_0}$  – Rolling moment coefficient at zero angle of attack  
 $C_{\ell\delta_\ell}$  – Derivative of the rolling moment coefficient due to the cant angle of fins  
 $C_{\ell_{00}}$  – Rolling moment coefficient due to the curvature of wrap-around fins  
 $\delta_\ell$  – Cant angle  
 $\alpha$  – Angle of attack

## Introduction

THE tube launcher requires folding wrap-around fins (WAF) which are deployed instantaneously after the missile left the tube of the launcher.

It was determined by the experimental data from the various wind tunnels that wrap-around fins develop the rolling moment even at zero angle of attack and zero cant angle of the fins. This moment has the direction to the centre of the curvature of the fins at subsonic speeds and changes the direction at supersonic speeds [1, 2, 3, 4, 5].

The value of this moment depends on the fins deployment angle, body diameter at the fins position relative to the missile caliber and the position of the fins section relative to the missile base.

Since the rolling moment of the missile with wrap-around fins is small, a special one-component transducer is designed in order to increase the accuracy of measurement

and to verify the measurement of the six-component strain gauge balance [6]. The experiments have shown that the rolling moment coefficients of the canted wrap-around fins are equal to the sum of the rolling moment coefficients due to the curvature of the wrap-around fins and the rolling moment coefficient of the canted equivalent flat fins [7].

The aerodynamic characteristics of the missiles with wrap-around fins are intensively calculated by computational fluid dynamics (CFD) [8],[9],[10] and [11]. The CFD results of the missile configuration with wrap-around fins in [8] show good agreement with the experimental data, but there is lack of accuracy in the roll moment and side force/moment determination. The calculated rolling moments for the laminar flow case with a three-dimensional full Navier-Stokes code show good agreement with the experimental data [9]. The flow field solutions of a wrap-around fin projectile calculated by three-dimensional Euler equations, with an accurately prepared grid, show good agreement with the experimental data [11].

The purpose of this paper is to present the results of the rolling moment coefficients of the missile with wrap-around fins and the equivalent flat fins calculated by the CFD software FLUENT (v12.0.16) and to compare the calculated values with the experimental data. The calculated and measured rolling moment coefficients of these two missile models are done for both zero cant angle of the fins and a cant angle equal to  $\delta_\ell = 0.8^\circ$ . Steady state calculations were used to compute the rolling moment coefficients of the missile models.

<sup>1)</sup> ROKETSAN Missile Industries Inc., P.K.:30, 06780 Elmadag-Ankara-TÜRKIYE

<sup>2)</sup> Military Technical Institute (VTI), Ratka Resanovića 1, 11132 Belgrade, SERBIA

### Missile Models Description

The basic dimensions of the missile model composed of a cylindrical body with an ogival nose and a wing section, are given in Fig.1.

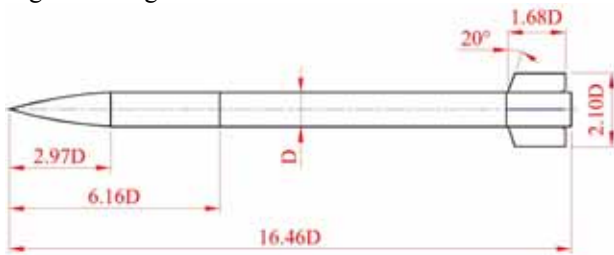


Figure 1. The basic dimensions of the model

The wing section of the model is designed so that wrap-around fins and flat fins can be easily interchanged and fixed to the cylindrical body. The flat fins are obtained by a projection of the wrap-around fins on the plane which goes through the longitudinal axis of the missile and the root chord of the wrap-around fins. The rear views of the WAF Model and the Flat-Fin Model are given in Fig.2.

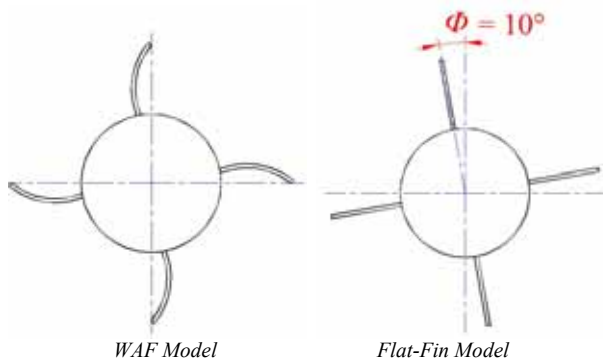


Figure 2. Rear view of the fins section

The design of the model permits also the interchange of two cylindrical bodies of the wing section so that two cant angles of the wings relative to the longitudinal axis can be obtained ( $\delta_i=0.0^\circ$  and  $\delta_i=0.8^\circ$ ).

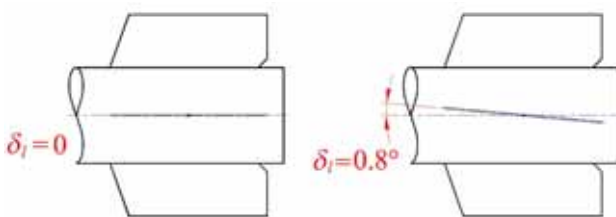


Figure 3. Cant angle of the fins

### CFD Simulation

Computational fluid dynamics was used to calculate the flow field around the missile models with wrap-around and flat fins in subsonic, transonic and supersonic flows. Computations were performed at Mach numbers ranging from 0.5 to 2.0 at zero degree angle of attack and the angle of attack from  $-10^\circ$  to  $10^\circ$  for Mach 0.7 and 2.0.

### Solid Model and Computational Mesh

Four different missile model geometries were generated for the CFD studies. For each model, two different fin sets with  $0^\circ$  and  $0.8^\circ$  cant angles were used. The generated solid models were shown in Fig.4 and 5.

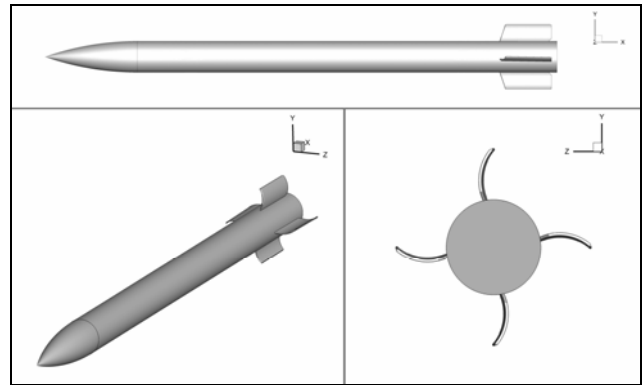


Figure 4. Solid model of the WAF Model

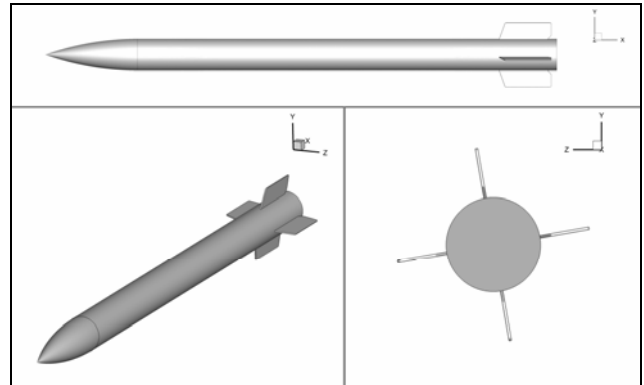


Figure 5. Solid model of the Flat-Fin Model

Both the solid model and the unstructured hybrid meshes were generated by the GAMBIT software package. The computational domain inlet was located 15 model body lengths upstream from the tip of the model nose and the computational domain outlet was located 24 model body lengths downstream from the model base.

In generating the meshes, the boundary layer mesh spacing was used near the model surface. The two-layer zonal model was used for the near-wall calculation and the first point off the surface was chosen to give  $y^+$  value close to 1. Twenty four layers of prismatic cells were generated to resolve the boundary layer adequately. The remaining part of the solution domain was completely composed of tetrahedral elements. The mesh growth rate was kept below 1.15. The cross-sectional views from the volume mesh and the surface mesh for the WAF Model and the Flat-Fin Model are shown in Fig.6 and 7, respectively.

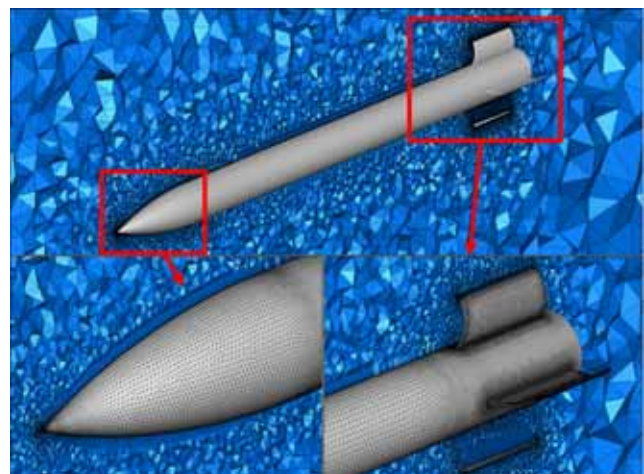
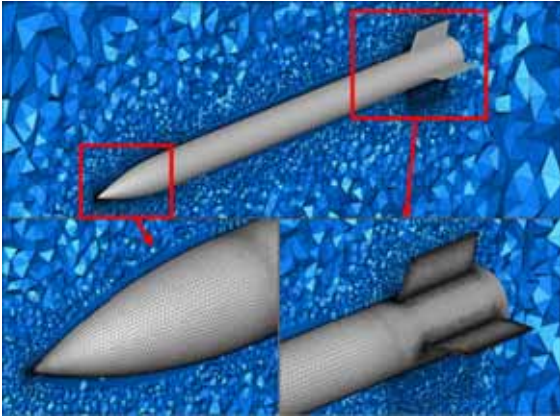
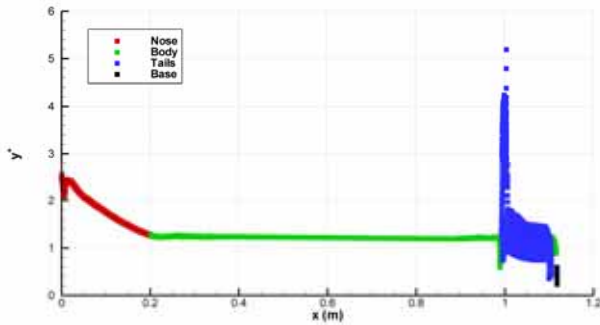


Figure 6. Surface and the computational domain grid for the WAF Model with zero cant angle



**Figure 7.** Surface and the computational domain grid for the Flat-Fin Model with zero cant angle

The post-processing of the converged results showed that the  $y^+$  value was in a range of 1.2-2.5 on the model nose, lower than 1 on the model base, 1.2 on the body and lower than 2 on the most of tail surfaces. Fig.8 shows the  $y^+$  values for the WAF Model at Mach number 2.0 and  $0^\circ$  angle of attack.



**Figure 8.**  $y^+$  values at Mach 2.0 for the Model-1 at zero degree angle of attack

### Flow Solver and Boundary Conditions

The FLUENT commercial flow solver was used to compute the rolling moments and the flow field around the wrap-around and flat finned missiles. The density-based, implicit, compressible, unstructured-mesh solver was used.

The coupled set of governing equations is discretized in time and time marching proceeds until a steady state solution is reached. In the implicit scheme, used in this study, an Euler implicit discretization in time is combined with a Newton-type linearization of the fluxes. Second-order discretization was used for all flow variables.

A modified form of the  $k-\varepsilon$  two-equation turbulence model (realizable  $k-\varepsilon$ ) was used in this study. This turbulence model solves transport equations for the turbulence kinetic energy,  $k$ , and its dissipation rate,  $\varepsilon$ . The term “realizable” means that the model satisfies certain mathematical constraints on the Reynolds stresses consistent with turbulent flow physics. The realizable  $k-\varepsilon$  model has shown substantial improvements over the standard  $k-\varepsilon$  model where flow features include strong streamline curvature, vortices, and rotation.

The effect of the turbulence model on the rolling moment coefficient is also investigated with the use of different turbulence models for a zero angle of attack case. The realizable  $k-\varepsilon$ ,  $k-\omega$  and Spallart-Allmaras turbulence models were used to compute a flow field around three models with the cant angle  $\delta_i=0.8^\circ$ .

The boundary conditions were as follows. Downstream,

upstream, and outer radial boundaries were set as far-field (characteristics-based inflow/outflow), with sea-level temperature and pressure free stream conditions (300 K, 101325 Pa). All solid surfaces were modeled as no-slip, adiabatic wall boundary conditions.

The model reference length is a model diameter of  $d=0.06788$  m and the reference area is the cross section of the missile body  $S=0.003619$  m<sup>2</sup>.

### CFD Solution Strategy

Viscous computational fluid dynamics simulations were performed in the ROKETSAN’s High Performance Computing (HPC) system. The 72 CPUs parallel supercomputer ORION was used for this study. The simulations were done with a maximum Courant-Friedrich-Lewy (CFL) number of 15 for all Mach numbers. Each case was started with a lower CFL value of 1.0 and ramped up to the maximum during the iterations of the simulation. The calculations took about 15–30 s of the CPU time per iteration and the convergence was achieved in about 4000-5000 iterations, depending on the Mach number, angle of attack and geometry. The convergence was determined by tracking the change in the flow residuals and the aerodynamic coefficients during the solution. The solution was deemed converged when the flow residuals were reduced for at least 3 orders of magnitude and the aerodynamic coefficients changed for less than about 1% over the last 100 iterations. Fig.9 shows the residual graph for the Mach number  $M=2.0$  and zero angle of attack  $\alpha=0^\circ$ .

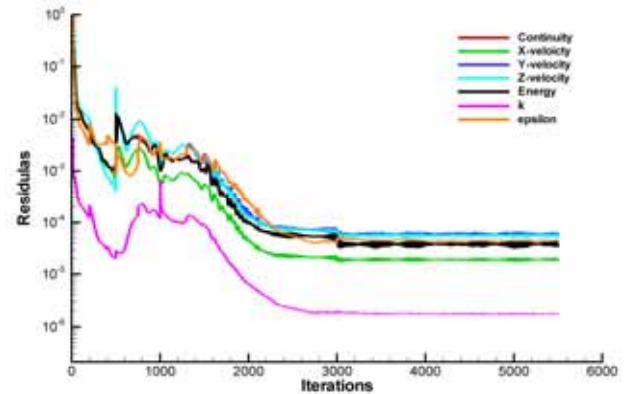


**Figure 9.** Residuals for Model-1 at Mach 2.0 and zero degree angle of attack

### Flow field Visualizations

To investigate the flow field characteristics of the WAF Model: oil-flow and streamline views are shown in Fig.10 and 11, respectively. These visualizations are performed for the angle of attack  $\alpha=10^\circ$  and Mach number  $M=0.7$ .

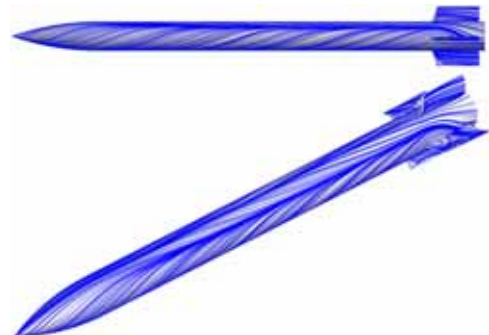


**Figure 10.** Surface flow for the WAF Model at Mach 0.7 and  $10^\circ$  degree angle of attack



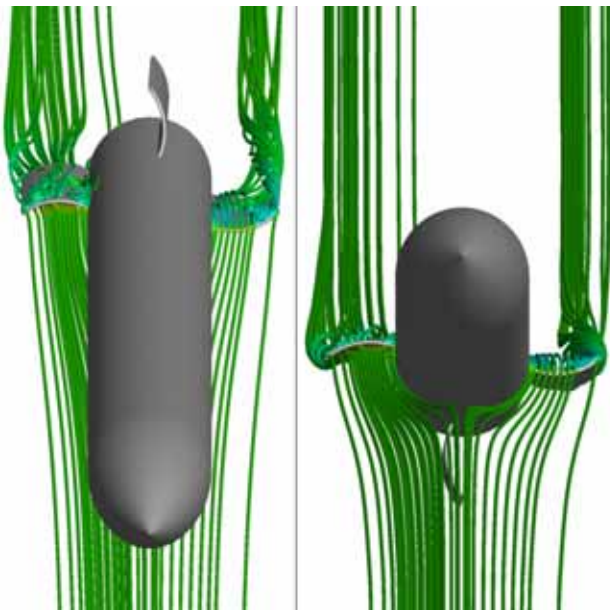


**Figure 11.** Streamlines for the WAF Model at Mach 0.7 and 10° degree angle of attack

**Rolling moment measurements**

The measurements of the rolling moments of the WAF Model and the Flat-Fin Model have been done in the blowdown-type pressurized wind tunnel T38 with a 1.5m x 1.5m square test section. The descriptions of the wind tunnel and the measurement equipment are given in [6].

The wind-tunnel measurements in the transonic region of Mach numbers have been done with porous walls inserted in the tunnel configuration. The porosity of walls can vary between 1.5% and 8%, depending on the Mach number, so as to achieve the best flow quality.

The model has been supported in the test section by a tail sting mounted on a pitch-and-roll mechanism by which desired aerodynamic angles can be achieved. The facility supports both the step-by-step model movement and the continuous movement of the model (“sweep”) during measurements. The positioning accuracy is 0.05° in pitch and 0.25° in roll.

The aerodynamic forces and moments acting on the model have been measured by a VTI40A internal six-component strain gauge balance. The range of the balance is 1130 N for axial force, 5000 N for side force, 10150 N for normal force, 184 Nm for the rolling moment, 530 Nm for the pitching moment and 256 for the yawing moment. The accuracy of this balance is approximately 0.20% of the full scale.

The measured rolling moment coefficients as a function of the Mach number and the angle of attack are given in [6] and [7].

**Comparison of the Calculated and Measured Rolling Moment Coefficients**

The diagrams of the calculated and measured roll moment coefficients with respect to the angle of attack for the WAF Model are given in Figs.12 – 13 for Mach numbers  $M = 0.7$  and  $M = 2.0$ , respectively.

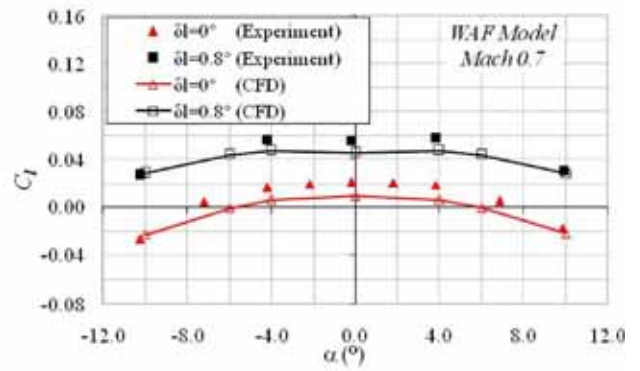


**Figure 12.** Comparisons of the experimental roll moment coefficients with the CFD results at Mach 0.7 for the WAF Model

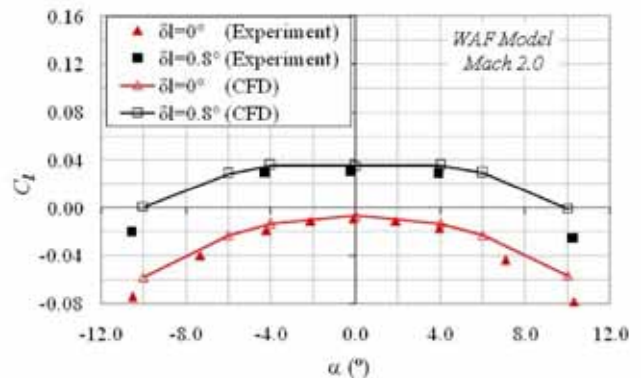


**Figure 13.** Comparisons of the experimental roll moment coefficients with the CFD results at Mach 2.0 for the WAF Model

Better agreements between the calculated and measured rolling moment coefficients of the WAF Model are obtained for  $M = 2.0$  than for  $M = 0.7$ . The calculated and measured rolling moment coefficients for two cant angles,  $\delta_\ell = 0^\circ$  and  $\delta_\ell = 0.8^\circ$ , at zero angle of attack

$\alpha = 0^\circ$  are given in Table 1 for  $M = 0.7$  and in Table 2 for  $M = 2.0$ . The differences between the calculated and measured rolling moment coefficients in percents are given in the same tables.

**Table 1.** WAF Model  $C_\ell$  for  $M = 0.7$  and  $\alpha = 0^\circ$

Fins cant angle	$\delta_\ell = 0^\circ$	$\delta_\ell = 0.8^\circ$
$C_{\ell(calculated)}$	0.009	0.0456
$C_{\ell(measured)}$	0.021	0.056
$\Delta C_\ell / C_{\ell(measured)}$	57.2 %	18.6 %

**Table 2.** WAF Model  $C_\ell$  for  $M = 2.0$  and  $\alpha = 0^\circ$

Fins cant angle	$\delta_\ell = 0^\circ$	$\delta_\ell = 0.8^\circ$
$C_{\ell(calculated)}$	-0.0068	0.0355
$C_{\ell(measured)}$	-0.0090	0.0310
$\Delta C_\ell / C_{\ell(measured)}$	24.4 %	14.5 %

The diagrams of the calculated and measured roll moment coefficients with respect to the angle of attack for the Flat-Fin Model are given in Figs.14 – 15 for Mach numbers  $M = 0.7$  and  $M = 2.0$ , respectively.

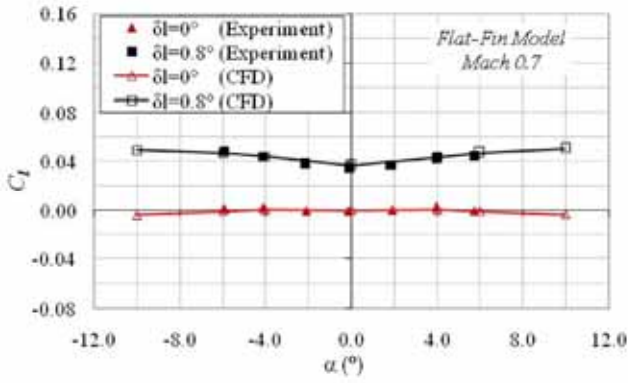


Figure 14. Comparisons of the experimental roll moment coefficients with the CFD results at Mach 0.7 for the Flat-Fin Model

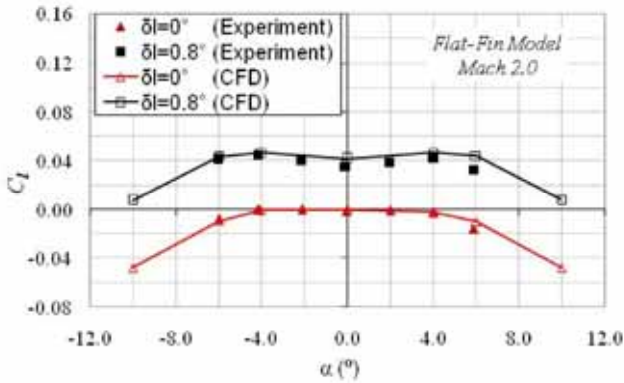


Figure 15. Comparisons of the experimental roll moment coefficients with the CFD results at Mach 2.0 for the Flat-Fin Model

The calculated and measured rolling moment coefficients for two cant angles  $\delta_\ell = 0^\circ$  and  $\delta_\ell = 0.8^\circ$  at zero angle of attack  $\alpha=0^\circ$  are given in Table 3 for  $M = 0.7$  and in Table 4 for  $M = 2.0$ . The differences between the calculated and measured rolling moment coefficients in percents are given in the same tables.

Table 3 Flat-Fin Model  $C_\ell$  for  $M = 0.7$  and  $\alpha = 0^\circ$

Fins cant angle	$\delta_\ell = 0^\circ$	$\delta_\ell = 0.8^\circ$
$C_{\ell(calculated)}$	0.002	0.0369
$C_{\ell(measured)}$	0.001	0.034
$\Delta C_\ell / C_{\ell(measured)}$	-	8.5%

Table 4 Flat-Fin Model  $C_\ell$  for  $M = 2.0$  and  $\alpha = 0^\circ$

Fins cant angle	$\delta_\ell = 0^\circ$	$\delta_\ell = 0.8^\circ$
$C_{\ell(calculated)}$	0.0001	0.0421
$C_{\ell(measured)}$	0.001	0.038
$\Delta C_\ell / C_{\ell(measured)}$	-	10.8%

The effect of the turbulence model on the rolling moment coefficients is also investigated for the missile models with the cant angle  $\delta_\ell = 0.8^\circ$  in Fig.16 and 17. The Spalart-Allmaras,  $k-\omega$  and Realizable  $k-\epsilon$  turbulence model results are compared with the experimental values for different Mach numbers from 0.5 to 2.0 at zero angle of attack. The Spalart-Allmaras turbulence model over-predicts the rolling moment coefficient for the Flat-Fin

Model, while the results for the WAF Model are very close to the experimental results. The Realizable  $k-\epsilon$  and  $k-\omega$  turbulence model results are similar to each other and capture the trend of the experimental results well. In the rest of the paper, the Realizable  $k-\epsilon$  turbulence model results are presented.

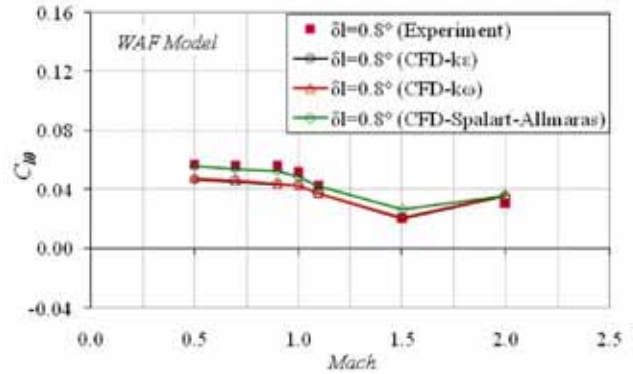


Figure 16. Effect of the turbulence model on the computational rolling moment coefficients for the WAF Model

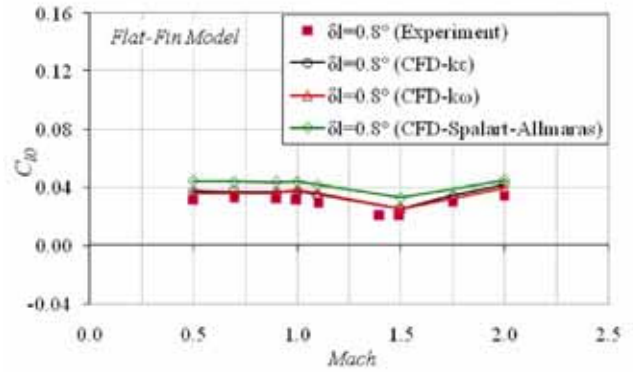


Figure 17. Effect of the turbulence model on the computational rolling moment coefficients for the Flat-Fin Model

The comparisons of the calculated and measured rolling moment coefficients for the WAF Model at zero degree angle of attack with respect to Mach numbers are shown in Fig.18. The CFD predictions compare very well to the measured  $C_{l_0}$ . The agreements between the calculated and measured rolling moment coefficients for the supersonic Mach numbers are better than for the subsonic Mach numbers.

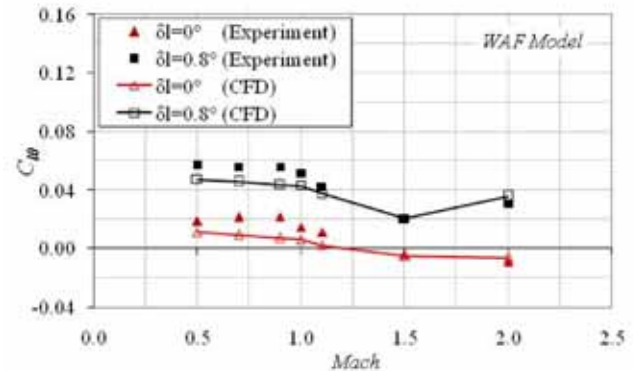
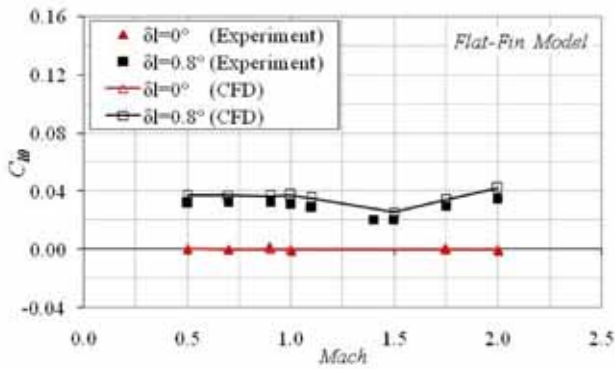


Figure 18. Comparisons of the experimental rolling moment coefficients with the CFD calculations at  $\alpha=0^\circ$  for the WAF Model

The comparisons of the calculated and measured rolling moment coefficients for the Flat-Fin Model at zero degree angle of attack as a function of Mach numbers are shown in Fig.19.



**Figure 19.** Comparisons of the experimental rolling moment coefficients with the CFD calculations at  $\alpha=0^\circ$  for the Flat-Fin Model

The rolling moment coefficients of the missile with canted flat fins at zero angle of attack can be written as a function of the can angle  $\delta_l$ .

$$C_{l0} = C_{l\delta_l} \delta_l \tag{1}$$

The derivative  $C_{l\delta_l}$  determined from the measured rolling moment coefficients in the wind tunnel and from the CFD calculation of the missile with canted flat fins as a function of Mach numbers is given in Fig.20.

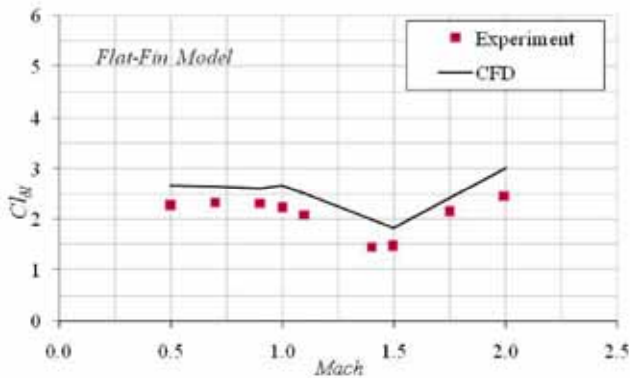


**Figure 20.** The derivative  $C_{l\delta_l}$  for the Flat-Fin Model as a function of Mach numbers

It can be seen that the rolling moment coefficient of missiles with WAF at zero angle of attack can be calculated summing the rolling moment coefficient due to the curvature of the fins and the rolling moment coefficient of canted equivalent flat fins.

$$C_{l0} = C_{l00} + C_{l\delta_l} \delta_l \tag{2}$$

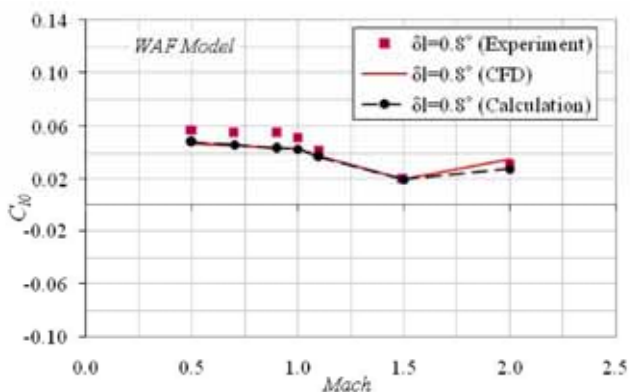


**Figure 21:** Comparisons of the experimental, computational and calculated roll moment coefficients for the WAF Model with  $\delta_l=0.8^\circ$  at  $\alpha=0^\circ$

The comparisons of the rolling moment coefficients of the missile model with wrap-around fins with the cant angle  $\delta_l = 0.8^\circ$  obtained by wind tunnel experiments, the CFD calculations and calculated by formula (2) are shown in Fig.21. The coefficients  $C_{l00}$  and  $C_{l\delta_l}$  used for the calculation of the rolling moment coefficients of the missile with canted wrap-around fins are obtained from the CFD results.

### Conclusion

The CFD calculations of the rolling moment coefficient by the FLUENT software package and the wind-tunnel measurements were performed for two missile models. One missile model is with wrap-around fins and the other missile model is with flat fins.

The wing section of the model is designed for a wind tunnel experiment so that wrap-around fins and flat fins can be easily interchanged and fixed to the cylindrical body. The flat fins are obtained by a projection of the wrap-around fins on the plane which goes through the longitudinal axis of the missile and the root chord of the wrap-around fins.

Four different missile model geometries were generated for the CFD studies. For each model, there are two cant angles of the fins relative to the missile axis ( $\delta_l = 0^\circ$  and  $\delta_l = 0.8^\circ$ ).

The effect of the CFD turbulence model on the rolling moment coefficients is also investigated for the missile models with the cant angle  $\delta_l = 0.8^\circ$ . The Spalart-Allmaras, k- $\omega$  and Realizable k- $\epsilon$  turbulence model results are compared with the experimental values for different Mach numbers from 0.5 to 2.0 at zero angle of attack. The Spalart-Allmaras turbulence model over-predicts the rolling moment coefficient for the Flat-Fin Model, while the results for the WAF Model are very close to the experimental results.

The difference between the calculated and measured rolling moment coefficients for the WAF Model is 14% in the supersonic regions and about 18% percents in the subsonic regions of Mach numbers for zero angle of attack  $\alpha = 0^\circ$  and cant angle  $\delta_l = 0.8^\circ$ . These differences are less than 10% for the Flat-Fin Model. The agreements between the calculated and measured rolling moment coefficients for the supersonic Mach numbers are better than for the subsonic Mach numbers.

The CFD calculations and the wind tunnel experiment have shown that the rolling moment coefficient of missiles with WAF at zero angle of attack is equal to the sum of the rolling moment coefficient of the canted equivalent flat fins and the rolling moment coefficient due to the curvature of the fins.

### References

- [1] *Design of aerodynamically stabilized free rockets* – Military Handbook MIL-HDBK-762 (MI) 17 July 1990
- [2] BAR-HAIM,B., SEGNER,A.: *Aerodynamics of Wrap-around Fins*, J. Spacecraft, July-August 1983, Vol.20, No.4.
- [3] CATANI,U., BERTIN,J.J., BOUSLOG,S.A.: *Aerodynamics Characteristics for a Slender Missile with Wrap-Around Fins*, Journal of Spacecraft and Rockets, March-April 1983, Vol.20, No.2, pp.122-128.
- [4] WINCHENBACH,G.L., BUFF,R.S., WHYTE,R.H., HATHAWAY,W.H.: *Subsonic and Transonic Aerodynamic of a Wrap-around Fin Configuration*, Journal of Guidance, Control, and Dynamics, 1986, Vol.9, No.6, pp.627-632.

- [5] TILMANN, C.P., HUFFMAN, R.E., Jr. BUTER, T.A., BOWERSOX, R.D.W.: Experimental Investigation of the Flow structure near a Single Wrap-around Fin, *Journal of Spacecraft and Rockets*, 1997, Vol.34, No.6, pp.729-736.
- [6] VITIĆ, A., SAMARĐIĆ, M., MARINKOVSKI, D.: *One Component Transducer for Measuring the Rolling Moment on the Missile Model*, Scientific Technical Review, ISSN 1820-0206, 2006, Vol.LVI, No.3-4, pp.82-86.
- [7] MANDIĆ, S.: *Analysis of the Rolling Moment Coefficients of a Rockets with Wrap-around Fins*, Scientific Technical Review, ISSN 1820-0206, 2006, Vol.LVI, No.2, pp.30-37.
- [8] WARDLAW, A.B., PRIOLO, F.J., SOLOMON, J.M.: *Multiple Zone Strategy for Supersonic Missiles*, *Journal of Spacecraft and Rockets*, July-August 1987, Vol.24, No.4.
- [9] EDGE, H.L.: *Computation of the Roll Moment for a Projectile with Wrap-around Fins*, *Journal of Spacecraft and Rockets*, July-August 1994, Vol.31, No.4.
- [10] BERNER, C., ABATE, G., DUPUIS, A.: *Aerodynamics of Wrap Around Fins using Experimental and Computational Techniques*, RTO AVT Symposium on Missile Aerodynamics, Sorrento, Italy, 1998.
- [11] SEUNG-KILL PEAK: *Computation of Roll Moment for a Projectile with Wrap-around Fins Using Euler Equation*, *Journal of Spacecraft and Rockets*, January-February 1999, Vol.36, No.1.
- [12] Fluent 12.0.16 Users Guide, Fluent, Inc.

Received: 02.11.2011.

## Analiza momenta valjanja rakete sa olučastim krilima primenom numeričke dinamike fluida i merenja u aerotunelu

Proračun momenta valjanja rakete primenom numeričke dinamike fluida i merenje u aerotunelu urađena su za dva modela. Jedan model rakete je sa olučastim krilima, a drugi sa ekvivalentnim pravim krilima. Cilj ovog rada je poređenje proračunskih vrednosti koeficijenta momenta valjanja sa izmerenim vrednostima u aerotunelu. Data je i analiza uticaja turbolentnog modela u programskom paketu FLUENT na tačnost proračuna momenta valjanja rakete. U radu je pokazano da se proračunske vrednosti aerodinamičkih koeficijenata momenta valjanja bolje poklapaju sa izmerenim vrednostima u supersonici u odnosu na subsoniku. Na osnovu izračunatih i izmerenih vrednosti koeficijenta momenta valjanja pokazano je da se moment valjanja rakete sa olučastim krilima može napisati kako zbir momenta valjanja stvorenog krivinom olučastih krila i momenta valjanja stvorenog uglom ugradnje ekvivalentnih pravih krila.

*Ključne reči:* aerodinamičko ispitivanje, aerodinamički proračun, aerodinamički moment, moment valjanja, raketa, pravo krilo, olučasto krilo, aerodinamički koeficijent, numerička dinamika fluida.

## Анализ момента прокатки ракеты с обернутыми вокруг крыльями с помощью численной динамики жидкостей (флуидов) и измерений в аэродинамической трубе

Расчёт момента прокатки ракеты с помощью численной динамики жидкостей и измерений в аэродинамической трубе были проведены на двух моделях. Одна модель ракеты с обернутыми вокруг крыльями и другая с эквивалентными прямыми крыльями. Целью данного исследования было сравнение расчётных значений коэффициента момента крена с результатами измерений в аэродинамической трубе. Здесь представлен и анализ воздействия турбулентной модели в пакете программного обеспечения FLUENT на точность расчёта крутящего момента прокатки ракеты. В настоящей работе показано, что расчётные значения аэродинамических коэффициентов момента прокатки лучше соответствуют измерениям в области сверхзвуковой аэродинамики, чем в области дозвуковой аэродинамики. Рассчитанные и измеренные значения коэффициента момента качания показали, что импульс прокатки ракеты с обернутыми вокруг крыльями можно представить в виде суммы переходящего момента, создаваемого плавниками кривой обернутых вокруг крыльев и момента качания, созданного углом монтажа эквивалентных прямых крыльев.

*Ключевые слова:* аэродинамические испытания, аэродинамический расчёт, аэродинамический момент, крутящий момент прокатки (момент крена), ракета, прямое крыло, обернутое вокруг крыло, аэродинамические коэффициенты, численная динамика жидкостей (динамика флуидов).

## **Analyse du moment de roulement du missile aux ailes enveloppées à l'aide de la dynamique numérique des fluides et par le mesurage dans la soufflerie aérienne**

Le calcul du moment de roulement chez le missile à l'aide de la dynamique numérique des fluides et le mesurage dans la soufflerie aérienne ont été faits pour deux modèles. Un modèle du missile a les ailes enveloppées tandis que l'autre modèle possède les ailes plates. Le but de ce travail est de comparer les valeurs obtenues pour les coefficients du moment de roulement avec les valeurs mesurées dans la soufflerie aérienne. On a présenté aussi l'analyse de l'influence du modèle turbulent par le progiciel FLUENT quant à la précision du calcul pour le moment de roulement du missile. On a démontré que les valeurs calculées des coefficients aérodynamiques du moments de roulement correspondaient mieux avec les valeurs mesurées dans la supersonique qu'à la subsonique. Se basant sur les valeurs mesurées et calculées pour les coefficients du moments de roulement on a démontré que le moment de roulement de missile aux ailes enveloppées pouvait être écrit comme la somme du moment de roulement dû à la courbature des ailes et du moment de roulement créé par l'angle des ailes plates équivalentes.

*Mots clés:* essai aérodynamique, calcul aérodynamique, moment aérodynamique, moment de roulement, missile, aile plate, aile enveloppée, coefficients aérodynamiques, dynamique numérique des fluides.